Paper

Unified Theory of Series, Parallel and LCL/CLC Resonant Circuits in Inductive Power Transfer and Capacitive Power Transfer

Hirono Namiki*a) Non-Member Takehiro Imura* Member Yoichi Hori* Fellow

This paper provides a general and systematic comparison of the transmission characteristics of series, parallel and LCL/CLC resonant circuits of both Inductive Power Transfer (IPT) and Capacitive Power Transfer (CPT) . The transmission characteristics are CC/CV characteristic, efficiency and output power when the power source is a voltage source or a current source. In terms of maximum efficiency, it was found to be common regardless of the transmission method or circuit. In terms of output power, it was found that when using a voltage source, high power was obtained by setting the transmitter side to S in IPT and the transmitter side to S or CLC in CPT. It was also found that when using a current source, high power was obtained by setting the transmitter side to P or LCL in IPT and the transmitter side to P in CPT. Furthermore, it was found that IPT obtains high power when the transmitter side circuit has the CV characteristic and CPT obtains high power when the transmitter side circuit has CC characteristic. In conclusion, S-S, S-LCL, LCL-S, LCL-P and LCL-LCL are superior in IPT and S-CLC, P-P, P-CLC, CLC-P, and CLC-CLC are superior in CPT.

Keywords : inductive power transfer, capacitive power transfer, transmission characteristics

1. Introduction

In recent years, as electronic devices have become more widespread and opportunities for charging have increased year by year. The problems with cable charging include lack of durability, risk of electric shock, cable deterioration and disconnection. Wireless Power Transfer (WPT) is a system that can transmit power without cables, and is expected to be widely used in portable devices, implantable medical devices, electric vehicles, robots, etc., due to its features such as freedom of location.

Inductive Power Transfer (IPT) and Capacitive Power Transfer (CPT) are non-radiative types of WPT. Both have advantage as transmission methods that can achieve higher transmission efficiency than the radiative type over transmission distances of up to several tens of centimetres.[1][2] The advantages of IPT are that it is easier to obtain higher power and longer transmission distances compared to CPT, while the advantages of CPT are that there is no risk of efficiency loss or heat generation due to metallic foreign objects, and lower cost and lighter weight due to the use of metal plates only. In the past, there are some studies that clarifies the characteristics of S-S, S-P, P-S and P-P, and among the four circuits, S-S and S-P are considered superior for both IPT and CPT.[3]-[5] Furthermore, in IPT, there are studies on advanced circuits with more compensation elements, such as LCL-LCL and double-LCC circuits.[6]-[9] There are also studies for selecting suitable circuits for the application, such as electric vehicles and medical equipment, etc.[10]-[14] Similarly, in CPT, there are studies comparing non-resonant circuits[15] , circuits with more compensation elements[16]-[22] and circuits with increased power transmission plates.[23]-[25] In addition, there are several studies study of circuit studies for high power, which is a challenge for CPT. [26]-[27] Furthermore, there are studies on WPT method that combines IPT and CPT[28] and a study comparing the characteristics of both IPT and CPT.[29]-[30]

The previous studies have shown that S-S and S-P are superior to both IPT and CPT, but these are comparisons based on one method only, and there are few publications that have made comprehensive and fair comparisons, including advanced circuits. The previous study compares resonant circuits as S, P and LCL, but no experiment and no qualitative studies.[31] It is also necessary to clarify the differences in transmission characteristics in order to guide the selection of the most suitable transmission method and circuit for the application.

Therefore, in this paper, the transmission characteristics compared by solving the circuit equations, which are the basis of electric circuits, to obtain the transmission characteristic equations and substituting the parameters of the unification conditions. The circuits to be compared are IPT and CPT, respectively, for the transmission and receiver sides as series resonance, parallel resonance and LCL/CLC resonance. The transmission characteristics are CC/CV characteristic, efficiency and output power when the power source is a voltage or current source. Unified conditions are compensation topology based on resonance phenomena, design method for compensation condition, loading condition, Q value, coupling coefficient k and power supply performance.

The remainder of the paper is made up as follows: in Chapter 2, the compared circuits are presented; in Chapters 3-5, the circuit equations for IPT and CPT respectively are solved for the transmission characteristics are derived. More specifically, in Chapter 3, CC/CV characteristic and compensation element conditions are determined; in Chapter 4, the efficiency and optimal load are determined; in Chapter 5, the output power is determined; in Chapter 6, a comparison of the calculated and simulated results is made to show the reliability of the calculations; in Chapter 7, the

a) Correspondence to: Hirono Namiki. E-mail: namiki.hirono21@gmail.com
* Tokyo University of Science, Imura-Hori Laboratory, 2639, Yamazaki, Noda, Chiba 278-0022, Japan

transmission characteristics are compared for each circuit and transmission method by fitting fair condition parameters to the various equations. Chapter 8 presents the qualitative study of the output power. Chapter 9 provides a comparison with experiments and Chapter 10 gives a conclusion.

2. Compared Circuits

2.1 Equivalent Circuit in IPT A typical transmission coil is shown in Fig. 1 and its structure can be shown by an equivalent circuit as shown in Fig. 2 (a). It can also be transformed into an equivalent T-shaped circuit as shown in Fig 2 (b). Here, the self-inductance and internal resistance of the transmitter coil are L_1 and r_1 respectively, while the self-inductance and internal resistance of the receiver coil are L_2 and r_2 respectively. The mutual inductance L_m, the coupling coefficient k representing the coupling between the transmitter and receiver and the Q values of the coils are defined as in equations (1) and (2).

$$L_m = k\sqrt{L_1 L_2} \quad \cdots\cdots (1)$$

$$Q_1 = \frac{\omega L_1}{r_1}, Q_2 = \frac{\omega L_2}{r_2} \quad \cdots\cdots (2)$$

2.2 Equivalent Circuit in CPT A typical transmitter and receiver capacitor consists of four plates as shown in Fig. 3. The self-capacitances C_1, C_2 and the mutual capacitance C_m can be expressed by equations (3)-(6), since each of the four plates is coupled to each other as shown in Fig. 4(a). Therefore, the π-type circuit can be represented as shown in Fig. 4.

$$C_1 = C_{12} + \frac{(C_{13}+C_{14})(C_{23}+C_{24})}{C_{13}+C_{14}+C_{23}+C_{24}} \quad \cdots\cdots (3)$$

$$C_2 = C_{34} + \frac{(C_{13}+C_{14})(C_{23}+C_{24})}{C_{13}+C_{14}+C_{23}+C_{24}} \quad \cdots\cdots (4)$$

$$C_m = \frac{C_{24}C_{13}-C_{14}C_{23}}{C_{13}+C_{14}+C_{23}+C_{24}} \quad \cdots\cdots (5)$$

$$C_m = k\sqrt{C_1 C_2} \quad \cdots\cdots (6)$$

2.3 Compared Circuits The compared circuits are shown in Fig. 5, 6. The circuits consist in IPT are a transmission coil with a resonant capacitor connected in series and in parallel. In addition, LCL in IPT is a circuit in which an additional inductor is placed in series in ahead or behind of P. The circuits consist in CPT are a transmission capacitor with a resonant coil connected in series (S) and in parallel (P). Moreover, CLC resonant in CPT is a circuit in which an additional capacitor in parallel in ahead or behind of S.

2.4 Configuration and Advantage of LCL/CLC As shown in Fig. 5, LCL circuit is a circuit in which an additional inductor is placed in series in ahead or behind of P in IPT and an additional capacitor in parallel in ahead or behind of S in CPT. The advantage of LCL circuits in IPT is that LCL-LCL circuits have the same excellent characteristics as S-S circuits and are also safer than S-S circuits when there is no receiver side. In the case of S-S, when there is no receiver side, the only resistance component is the internal resistance of the coil due to series resonance, which causes a large current to flow, which is dangerous. However, when the transmitter side is LCL, the input impedance is large so that few current flows in the transmitter side circuit, making it safe.

As there is no commonly recognised and established LCL or CLC circuit in CPT. Therefore, a circuit is selected and defined that corresponds to the LCL circuit in IPT as CLC, in this paper. In addition, CLC is considered to be able to obtain high power because of the transmitter side circuit's CC characteristics. The reasons why CC characteristics of the transmitter side can obtain high power are discussed in detail in Chapter 8.

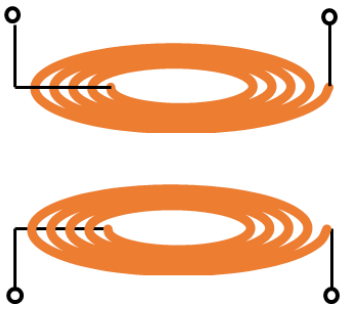

Fig. 1. Transmitter coil.

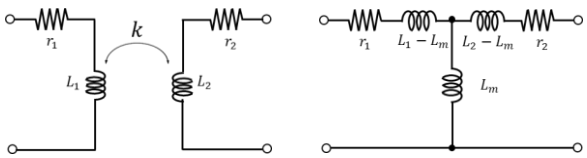

(a) Coupled circuit (a) Figure T type circuit

Fig. 2. Equivalent circuit in IPT.

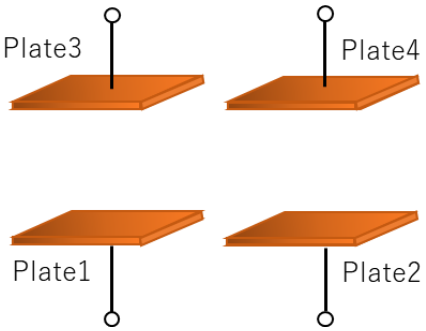

Fig. 3. Transmitter coupler.

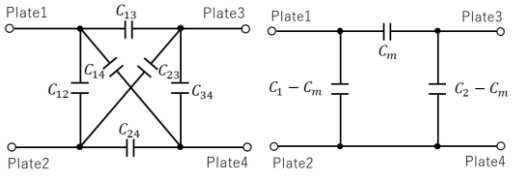

(a) Coupled circuit (a) Figure π type circuit

Fig. 4. Equivalent circuit in CPT.

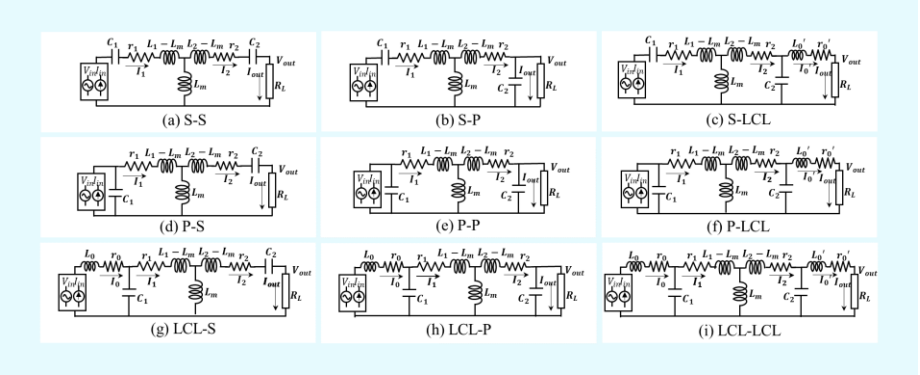

Fig. 5. Compared circuit in IPT.

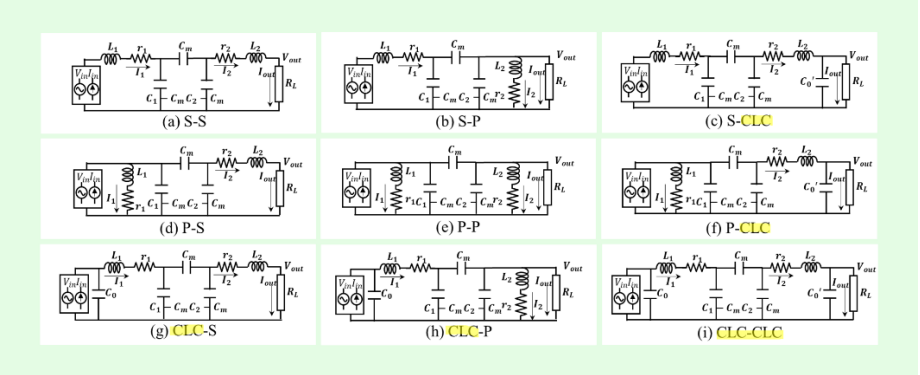

Fig. 6. Compared circuit in CPT.

3. Compensation Condition and CC/CV Characteristic

3.1 How to Design for Compensation Condition In this chapter, the compensation condition and CC/CV characteristics of resistance load are derived. The compensation elements are resonant capacitors in IPT and resonant inductors in CPT, which can achieve high efficiency and high power by appropriate design. In this paper, the values of reactance compensation elements are determined by a design method based on gyrator or ideal transformer characteristic. The design method based on gyrator or ideal transformer characteristic is a design method in which the F parameter of a two-terminal pair circuit such as equation (7) and Fig. 7 are set to $A = D = 0$ or $B = C = 0$ under the condition that $r_1 = r_2 = 0$, so that high-efficiency transmission can be achieved. The gyrator characteristic has CC characteristic when a voltage source is connected and CV characteristic when a current source is connected, according to equation (8). The ideal transformer characteristic has CV characteristic when a voltage source is connected and CC characteristic when a current source is connected, according to equation (9).

$$\begin{bmatrix} V_{in} \\ I_{in} \end{bmatrix} = \begin{bmatrix} A & B \\ C & D \end{bmatrix} \begin{bmatrix} V_{out} \\ I_{out} \end{bmatrix} \quad \cdots\cdots (7)$$

$$\begin{bmatrix} V_{in} \\ I_{in} \end{bmatrix} = \begin{bmatrix} 0 & B \\ C & 0 \end{bmatrix} \begin{bmatrix} V_{out} \\ I_{out} \end{bmatrix} \quad \cdots\cdots (8)$$

$$\begin{bmatrix} V_{in} \\ I_{in} \end{bmatrix} = \begin{bmatrix} A & 0 \\ 0 & D \end{bmatrix} \begin{bmatrix} V_{out} \\ I_{out} \end{bmatrix} \quad \cdots\cdots (9)$$

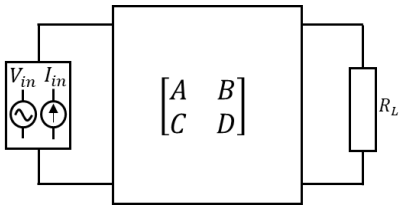

Fig. 7. Two-terminal pair circuit.

3.2 Compensation Condition and CC/CV Characteristic in IPT The F parameter of LCL-LCL circuit can be expressed as in equation (10).

$$\begin{cases} A = \frac{1}{\omega L_m}[\omega\{L_0 + L_1(1-\omega^2 L_0 C_1)\}(1-\omega^2 L_2 C_2) + \omega^3 L_m^2 C_2(1-\omega^2 L_0' C_2)] \\ B = \frac{j\omega}{L_m}[\{L_0 + L_1(1-\omega^2 L_0 C_1)\}\{L_2 + L_0'(1-\omega^2 L_2 C_2)\} - L_m^2(1-\omega^2 L_0 C_1)(1-\omega^2 L_0' C_2)] \\ C = \frac{j}{\omega L_m}\{-(1-\omega^2 L_0 C_1)(1-\omega^2 L_0 C_1) + \omega^4 L_m^2 C_1 C_2\} \\ D = \frac{1}{\omega L_m}[(1-\omega^2 L_1 C_1)\omega\{L_2 + L_0'(1-\omega^2 L_2 C_2)\} + \omega^3 L_m^2 C_1(1-\omega^2 L_0' C_2)] \end{cases} \quad \cdots\cdots (10)$$

By proper design of the compensation capacitor $A = D = 0$ and it is possible to satisfy C_1, C_2 is as in equation (11). Furthermore, by applying the compensation conditions of equation (11) to equation (10), the F parameter can be expressed as in equation (12).

$$C_1 = \frac{1}{\omega^2 L_1} = \frac{1}{\omega^2 L_0}, C_2 = \frac{1}{\omega^2 L_2} = \frac{1}{\omega^2 L_0'} \quad \cdots\cdots (11)$$

$$\begin{bmatrix} V_{in} \\ I_{in} \end{bmatrix} = \begin{bmatrix} 0 & \frac{j\omega L_0 L_2}{L_m} \\ j\omega^3 L_m C_1 C_2 & 0 \end{bmatrix} \begin{bmatrix} V_{out} \\ I_{out} \end{bmatrix} \quad \cdots\cdots (12)$$

Table 1. Compensation capacitance condition in IPT.

Circuit	C_1	C_2
S-S	$C_1 = \frac{1}{\omega^2 L_1}$	$C_2 = \frac{1}{\omega^2 L_2}$
S-P	$C_1 = \frac{1}{\omega^2 (1-k^2) L_1}$	$C_2 = \frac{1}{\omega^2 L_2}$
S-LCL	$C_1 = \frac{1}{\omega^2 L_1}$	$C_2 = \frac{1}{\omega^2 L_2} = \frac{1}{\omega^2 L_0'}$
P-S	$C_1 = \frac{1}{\omega^2 L_1}$	$C_2 = \frac{1}{\omega^2 (1-k^2) L_2}$
P-P	$C_1 = \frac{1}{\omega^2 (1-k^2) L_1}$	$C_2 = \frac{1}{\omega^2 (1-k^2) L_2}$
P-LCL	$C_1 = \frac{1}{\omega^2 L_1}$	$C_2 = \frac{1}{\omega^2 L_2} = \frac{1}{\omega^2 L_0'}$
LCL-S	$C_1 = \frac{1}{\omega^2 L_1} = \frac{1}{\omega^2 L_0}$	$C_2 = \frac{1}{\omega^2 L_2}$
LCL-P	$C_1 = \frac{1}{\omega^2 L_1} = \frac{1}{\omega^2 L_0}$	$C_2 = \frac{1}{\omega^2 L_2}$
LCL-LCL	$C_1 = \frac{1}{\omega^2 L_1} = \frac{1}{\omega^2 L_0}$	$C_2 = \frac{1}{\omega^2 L_2} = \frac{1}{\omega^2 L_0'}$

Table 2. CC/CV characteristic in IPT.

Circuit	Voltage Source	Current Source
S-S	CC	CV
S-P	CV	CC
S-LCL	CV	CC
P-S	CV	CC
P-P	CC	CV
P-LCL	None	CV
LCL-S	CV	CC
LCL-P	CC	None
LCL-LCL	CC	CV

Since it has gyrator characteristics from equation (12), it has CC characteristics when the power supply is a voltage source and CV characteristics when it is a current source.

Table 1 and 2 show the results of the compensation condition and CC/CV characteristics for the other circuits in IPT. The compensation conditions of S-P, P-S and P-P circuits depend on the coupling coefficient k. Therefore, it is not suitable when the coupling coefficient varies. Table 2. shows that P-LCL and LCL-P do not have CC/CV characteristic depending on the type of power source, while the other circuits have CC/CV characteristic regardless of the type of power source.

3.3 Compensation Condition and CC/CV Characteristic in CPT The F parameters of CLC-CLC circuit can be expressed as in equation (13).

$$\begin{cases} A = \frac{1}{\omega C_m}[\omega^3 L_1 C_m^2 (1-\omega^2 L_2 C_0') + (1-\omega^2 L_1 C_1)\{\omega C_2 + \omega C_0'(1-\omega^2 L_2 C_2)\}] \\ B = \frac{j}{\omega C_m}\{\omega^4 L_1 L_2 C_m^2 - (1-\omega^2 L_1 C_1)(1-\omega^2 L_2 C_2)\} \\ C = \frac{j\omega}{C_m}[-C_m^2 (1-\omega^2 L_1 C_0)(1-\omega^2 L_2 C_0') + \{C_0 + C_1(1-\omega^2 L_1 C_0)\}\{C_2 + C_0'(1-\omega^2 L_2 C_2)\}] \\ D = \frac{1}{\omega C_m}[\omega^3 L_2 C_m^2 (1-\omega^2 L_1 C_0) + \omega\{C_0 + C_1(1-\omega^2 L_1 C_0)\}(1-\omega^2 L_2 C_2)] \end{cases} \quad \cdots\cdots (13)$$

Table 3. Compensation Inductance condition in CPT.

Circuit	L_1	L_2
S-S	$L_1 = \frac{1}{\omega^2 (1-k^2) C_1}$	$L_2 = \frac{1}{\omega^2 (1-k^2) C_2}$
S-P	$L_1 = \frac{1}{\omega^2 C_1}$	$L_2 = \frac{1}{\omega^2 (1-k^2) C_2}$
S-CLC	$L_1 = \frac{1}{\omega^2 C_1}$	$L_2 = \frac{1}{\omega^2 C_2} = \frac{1}{\omega^2 C_0'}$
P-S	$L_1 = \frac{1}{\omega^2 (1-k^2) C_1}$	$L_2 = \frac{1}{\omega^2 C_2}$
P-P	$L_1 = \frac{1}{\omega^2 C_1}$	$L_2 = \frac{1}{\omega^2 C_2}$
P-CLC	$L_1 = \frac{1}{\omega^2 C_1}$	$L_2 = \frac{1}{\omega^2 C_2} = \frac{1}{\omega^2 C_0'}$
CLC-S	$L_1 = \frac{1}{\omega^2 C_1} = \frac{1}{\omega^2 C_0}$	$L_2 = \frac{1}{\omega^2 C_2}$
CLC-P	$L_1 = \frac{1}{\omega^2 C_1} = \frac{1}{\omega^2 C_0}$	$L_2 = \frac{1}{\omega^2 C_2}$
CLC-CLC	$L_1 = \frac{1}{\omega^2 C_1} = \frac{1}{\omega^2 C_0}$	$L_2 = \frac{1}{\omega^2 C_2} = \frac{1}{\omega^2 C_0'}$

Table 4. CC/CV characteristic in CPT.

Circuit	Voltage Source	Current Source
S-S	CC	CV
S-P	CV	CC
S-CLC	CC	None
P-S	CV	CC
P-P	CC	CV
P-CLC	CV	CC
CLC-S	None	CV
CLC-P	CV	CC
CLC-CLC	CC	CV

By proper design of the compensation inductor $A = D = 0$ and it is possible to satisfy L_1, L_2 is as in equation (14). Furthermore, the F parameter can be represented as in equation (15).

$$L_1 = \frac{1}{\omega^2 C_1} = \frac{1}{\omega^2 C_0}, L_2 = \frac{1}{\omega^2 C_2} = \frac{1}{\omega^2 C_0'} \quad \cdots\cdots (14)$$

$$\begin{bmatrix} V_{in} \\ I_{in} \end{bmatrix} = \begin{bmatrix} 0 & j\omega^3 L_1 L_2 C_m \\ \frac{j\omega C_0 C_2}{C_m} & 0 \end{bmatrix} \begin{bmatrix} V_{out} \\ I_{out} \end{bmatrix} \quad \cdots\cdots (15)$$

Since it has gyrator characteristics from equation (15), it has CC characteristics when the power supply is a voltage source and CV characteristics when it is a current source. Table 3 and 4 show the results obtained for the compensation condition and CC/CV characteristic for the other circuits of CPT. Table 3. shows that S-S, S-P and P-S circuits have the disadvantage that compensation condition depends on the coupling coefficient k. Table 4. shows that S-CLC and CLC-S do not have CC/CV characteristic depending on the type of power source, while the other circuits have CC/CV characteristic regardless of the type of power source.

4. Efficiency and Optimal Load

In this chapter, the equations for efficiency and optimal load for each circuit are derived. The equations for efficiency and optimal load do not depend on the type of power supply. The reason is that the value of power supply does not affect the efficiency when load resistance is used, and the input voltage V_{in} and input current I_{in} have and the relationship is as shown in equation (16) by using the input impedance Z_{in}.

$$|V_{in}| = |Z_{in}||I_{in}| \quad \cdots\cdots (16)$$

Therefore, since voltage and current sources are interchangeable, it can be said that the efficiency is independent of the type of power supply and the optimal load determined from the efficiency is also independent of the type of power supply.

4.1 Efficiency and Optimal Load in IPT

The loop currents I_{l0}, I_{l1}, I_{l2} and impedance Z for LCL-LCL in IPT are set as shown in Fig. 8. The circuit equation of the circuit is as in equation (17). Here, equation (17) shows the form in which the diagonal components are organised by applying the compensation conditions presented in equation (11).

$$\begin{bmatrix} V_{in} \\ 0 \\ 0 \end{bmatrix} = \begin{bmatrix} r_0 & -\frac{1}{j\omega C_1} & 0 \\ -\frac{1}{j\omega C_1} & r_1 & -j\omega L_m \\ 0 & -j\omega L_m & r_2 + \frac{L_0'}{C_2(r_0'+R_L)} \end{bmatrix} \begin{bmatrix} I_{l0} \\ I_{l1} \\ I_{l2} \end{bmatrix} \quad \cdots\cdots (17)$$

As the matrix determinant defines Δ, the currents are as in equations (18)-(21).

$$I_0 = I_{l0} = \frac{V_{in}}{\Delta}\left[r_1\left\{r_2 + \frac{L_0'}{C_2(r_0'+R_L)}\right\} + \omega^2 L_m^2\right] \quad \cdots\cdots (18)$$

$$I_1 = I_{l1} = \frac{V_{in}}{\Delta}\frac{1}{j\omega C_1}\left\{r_2 + \frac{L_0'}{C_2(r_0'+R_L)}\right\} \quad \cdots\cdots (19)$$

$$I_2 = I_{out} = I_{l3} = \frac{V_{in}}{\Delta}\frac{L_m}{C_1} \quad \cdots\cdots (20)$$

$$I_0' = I_{out} = \frac{ZI_{l2}}{r_0'+R_L+j\omega L_0'} = \frac{V_{in}}{\Delta}\frac{L_m}{j\omega C_1 C_2(r_0'+R_L)} \quad \cdots\cdots (21)$$

Since the efficiency can be obtained from equation (22), equation (25) can be obtained from the ratio equation as in equation (24) and the Q-value equation as in equation (23). Here, $r_0 = r_1, r_2 = r_0'$ to match the Q values.

$$\eta = \frac{R_L|I_{out}|^2}{r_0|I_0|^2 + r_1|I_1|^2 + r_2|I_2|^2 + R_L|I_{out}|^2} \quad \cdots\cdots (22)$$

$$Q_1 = \frac{\omega L_0}{r_0} = \frac{\omega L_1}{r_1} = \frac{1}{\omega C_1 r_1}, Q_2 = \frac{\omega L_2}{r_2} = \frac{\omega L_0'}{r_0'} = \frac{1}{\omega C_2 r_2} \quad \cdots\cdots (23)$$

$$r_0|I_0|^2 : r_1|I_1|^2 : r_2|I_2|^2 : R_L|I_{out}|^2 = r_0\left\{\left(1 + \frac{Q_2^2 r_2}{r_0'+R_L}\right) + k^2 Q_1 Q_2\right\}^2 : Q_1^2 r_1\left(1 + \frac{Q^2 r_2}{r_0'+R_L}\right)^2 : k^2 Q_1^3 Q_2 r_1 : \frac{k^2 Q_1^3 Q_2^3 r_1 r_2 R_L}{(r_0'+R_L)^2} \quad \cdots\cdots (24)$$

$$\eta^{LCL-LCL} = \frac{k^2 Q_1^3 Q_2^3 r_2 R_L}{\left[\{(1+Q_1^2)(1+Q_2^2) + k^2 Q_1 Q_2\} r_2 + (1+ + Q_1^2 + k^2 Q_1 Q_2) R_L\right] \{(1+Q_2^2 + k^2 Q_1 Q_2) r_2 + (1 + k^2 Q_1 Q_2) R_L\}} \quad \cdots\cdots (25)$$

In the same way, the efficiency of the other circuits of IPT can be obtained in the same way, as shown in Table 5.

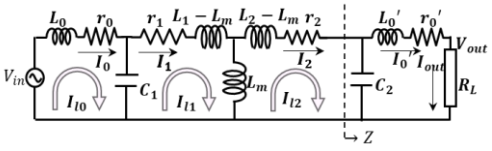

Fig. 8. LCL-LCL circuit in IPT.

Table 5. Efficiency in IPT.

Circuit	Efficiency
S-S	$\frac{k^2 Q_1 Q_2 r_2 R_L}{\{(1+k^2 Q_1 Q_2) r_2 + R_L\}(r_2 + R_L)}$
S-P	$\frac{k^2(1-k^2)^2 Q_1 Q_2^3 ((1-k^2)^2 Q_2^2 r_2^2 + R_L^2) r_2 R_L}{\{(1-k^2)^2 Q_2^2 r_2^2 + R_L^2 + (1-k^2)^2 Q_2^2 r_2 R_L\}} \{(1+k^2 Q_1 Q_2)\{(1-k^2)^2 Q_2^2 r_2^2 + R_L^2\} + (1-k^2)^2 Q_2^2 r_2 R_L\} + Q_2^2\{(1-k^2)^2 Q_2^2 r_2^2 + k^2 R_L^2\}^2$
S-LCL	$\frac{k^2 Q_1 Q_2^3 r_2 R_L}{\{(1+Q_2^2) r_2 + R_L\}\{(1+Q_2^2 + k^2 Q_1 Q_2) r_2 + (1+k^2 Q_1 Q_2) R_L\}}$
P-S	$\frac{k^2 Q_1 Q_2 r_2 R_L}{\{(1+k^2 Q_1 Q_2) r_2 + R_L\}(r_2 + R_L) + k^4 Q_2^2 r_2^2}$
P-P	$\frac{k^2(1-k^2)^2 Q_1 Q_2^3 r_2 R_L \{(1-k^2)^2 Q_2^2 r_2^2 + R_L^2\}}{\{(1-k^2)^2 Q_2^2 r_2 (r_2 + R_L) + R_L^2\}} [(1+k^2 Q_1 Q_2)\{(1-k^2)^2 Q_2^2 r_2^2 + R_L^2\} + (1-k^2)^2 Q_2^2 r_2 R_L] + Q_2^2\{(1-k^2)^2 Q_2^2 r_2^2 + k^2 R_L^2\}^2$
P-LCL	$\frac{k^2 Q_1 Q_2^3 r_2 R_L}{\{(1+Q_2^2) r_2 + R_L\}\{(1+Q_2^2 + k^2 Q_1 Q_2) r_2 + (1+k^2 Q_1 Q_2) R_L\}}$
LCL-S	$\frac{k^2 Q_1^3 Q_2 r_2 R_L}{\{(1+k^2 Q_1 Q_2) r_2 + R_L\}\{(1+Q_1^2 + k^2 Q_1 Q_2) r_2 + (1+Q_1^2) R_L\}}$
LCL-P	$\frac{k^2 Q_1^3 Q_2^2 r_2 R_L}{\{(1+Q_1^2 + k^2 Q_1 Q_2)\}} \{(1+k^2 Q_1 Q_2)(Q_2^2 r_2^2 + R_L^2) + Q_2^2 r_2 R_L\} + (1+Q_1^2) Q_2^2 r_2 \{Q_2^2 r_2 + (1+k^2 Q_1 Q_2) R_L\}$
LCL-LCL	$\frac{k^2 Q_1^3 Q_2^3 r_2 R_L}{[\{(1+Q_1^2)(1+Q_2^2) + k^2 Q_1 Q_2\} r_2 + (1 + + Q_1^2 + k^2 Q_1 Q_2) R_L]} \{(1+Q_2^2 + k^2 Q_1 Q_2) r_2 + (1+k^2 Q_1 Q_2) R_L\}$

In LCL-LCL circuits the optimal load to achieve maximum efficiency R_{Lopt} is expressed in equation (27) by applying the differential equation in equation (26) to equation (25).

$$\frac{\partial \eta}{\partial R_L} = 0 \quad \cdots\cdots (26)$$

$$R_{Lopt}^{LCL-LCL} = r_2\sqrt{\frac{(1+Q_2^2+k^2 Q_1 Q_2)\{(1+Q_1^2)(1+Q_2^2)+k^2 Q_1 Q_2\}}{(1+k^2 Q_1 Q_2)(1+Q_1^2+k^2 Q_1 Q_2)}} \quad \cdots\cdots (27)$$

Similarly, for the other circuits is calculated as shown in Table 6.

Table .6 Optimal Load in IPT.

Circuit	Optimal Load
S-S	$r_2\sqrt{1+k^2 Q_1 Q_2}$
S-P	$(1-k^2) Q_2 r_2 \sqrt{\frac{1+Q_2^2+k^2 Q_1 Q_2}{1+k^2 Q_1 Q_2 + k^4 Q_2^2}}$
S-LCL	$r_2\sqrt{\frac{(1+Q_2^2)(1+Q_2^2+k^2 Q_1 Q_2)}{1+k^2 Q_1 Q_2}}$
P-S	$r_2\sqrt{1+k^2 Q_1 Q_2 + k^4 Q_2^2}$
P-P	$(1-k^2) Q_2 r_2 \sqrt{\frac{1+Q_2^2+k^2 Q_1 Q_2}{1+k^2 Q_1 Q_2 + k^4 Q_2^2}}$
P-LCL	$r_2\sqrt{\frac{(1+Q_2^2)(1+Q_2^2+k^2 Q_1 Q_2)}{1+k^2 Q_1 Q_2}}$
LCL-S	$r_2\sqrt{\frac{(1+k^2 Q_1 Q_2)(1+Q_1^2+k^2 Q_1 Q_2)}{1+Q_1^2}}$
LCL-P	$Q_2 r_2\sqrt{\frac{(1+k^2 Q_1 Q_2)(1+Q_1^2+k^2 Q_1 Q_2)+(1+Q_1^2) Q_2^2}{(1+k^2 Q_1 Q_2)(1+Q_1^2+k^2 Q_1 Q_2)}}$
LCL-LCL	$r_2\sqrt{\frac{(1+Q_2^2+k^2 Q_1 Q_2)\{(1+Q_1^2)(1+Q_2^2)+k^2 Q_1 Q_2\}}{(1+k^2 Q_1 Q_2)(1+Q_1^2+k^2 Q_1 Q_2)}}$

4.2 Efficiency and Optimal Load in CPT Similarly for CPT, the efficiency can be obtained by solving the circuit equation by applying the compensation conditions. Here, for simplicity, the circuit equation is made as in Fig. 9 using current source-voltage source conversion. As the loop currents I_{l1}, I_{lm}, I_{l2} and impedance Z for CLC-CLC in CPT are set as shown in Fig. 9 (b) , the circuit equation is as in equation (28). Here, C_1', C_2' is placed in equation (29).

$$\begin{bmatrix} V_{in}' \\ 0 \\ 0 \end{bmatrix} = \begin{bmatrix} r_1 + \frac{C_1 - C_m + \omega^2 L_1 C_0 C_m}{j\omega C_0 C_1'} & \frac{1}{j\omega C_1'} & 0 \\ -\frac{1}{j\omega C_1'} & \frac{C_1 C_2 - C_m^2}{j\omega C_1' C_2' C_m} & -\frac{1}{j\omega C_2'} \\ 0 & -\frac{1}{j\omega C_2'} & r_2 + \frac{\omega^2 L_2 C_m + j\omega C_2 R_L}{j\omega C_2'(1 + j\omega C_0' R_L)} \end{bmatrix} \begin{bmatrix} I_{l1} \\ I_{lm} \\ I_{l2} \end{bmatrix} \cdot \quad (28)$$

$$C_1' = C_1 - C_m, C_2' = C_2 - C_m \quad (29)$$

As the matrix determinant defines Δ, the currents are as in equations (30)-(32).

$$I_1 = I_{l1} = \frac{V_{in}'}{\Delta}\left[\frac{C_1 C_2 - C_m^2}{j\omega C_1' C_2' C_m}\left\{r_2 + \frac{\omega^2 L_2 C_m + j\omega C_2 R_L}{j\omega C_2'(1 + j\omega C_0' R_L)}\right\} + \frac{1}{\omega^2 C'^2_2}\right] \quad (30)$$

$$I_2 = I_{l2} = \frac{V_{in}'}{\Delta}\left\{-\frac{1}{\omega^2 C_1' C_2'}\right\} \quad (31)$$

$$I_{out} = \frac{ZI_{l2}}{R_L} = \frac{V_{in}'}{\Delta}\left\{-\frac{1}{\omega^2 C_1' C_2'(1 + j\omega C_0' R_L)}\right\} \quad (32)$$

Since the efficiency can be obtained from equation (22), the ratio of each can be taken as in equation (33), and the efficiency can be expressed as in equation (34) using Q_1, Q_2 of resonant coils as equation (2).

$$\begin{aligned} & r_1|I_1|^2 : r_2|I_2|^2 : R_L|I_{out}|^2 \\ & = \left(\frac{R_L^2}{Q_1 Q_2^2 r_1 r_2^2} + \frac{k^2}{Q_1 r_1}\right)^2 \left(\frac{Q_2^2 r_2^2}{Q_2^2 r_2^2 + R_L^2}\right)^2 + \frac{(1-k^2)^2}{Q_1^2 Q_2^2 r_1^2 r_2^2}\left(r_2 + \frac{Q_2^2 r_2^2 R_L}{Q_2^2 r_2^2 + R_L^2}\right)^2 \\ & : \frac{k^2}{Q_1 Q_2 r_1 r_2} : \frac{k^2}{Q_1 Q_2 r_1 r_2}\frac{Q_2^2 r_2^2 R_L}{Q_2^2 r_2^2 + R_L^2} \end{aligned} \quad (33)$$

$$\eta^{CLC-CLC} = \frac{k^2 Q_1 Q_2^3 r_2 R_L}{\{(1-k^2)^2 + k^2 Q_1 Q_2\}\{Q_2^2 r_2 (r_2 + R_L) + R_L^2\} + Q_2^2\{k^4 Q_2^2 r_2^2 + (1-k^2)^2 r_2 R_L + R_L^2\}} \quad (34)$$

Similarly, the efficiencies for the other circuits in CPT can be obtained as shown in Table 7.

The optimal load to achieve maximum efficiency in CLC-CLC circuit R_{Lopt} is expressed in equation (35) by applying the differential equation in equation (26) to equation (34).

$$R_{Lopt}^{CLC-CLC} = Q_2 r_2 \sqrt{\frac{(1-k^2)^2 + k^4 Q_2^2 + k^2 Q_1 Q_2}{(1-k^2)^2 + Q_2^2 + k^2 Q_1 Q_2}} \quad (35)$$

From the above, the results of the optimal load for the other circuits in CPT are as shown in Tabe 8.

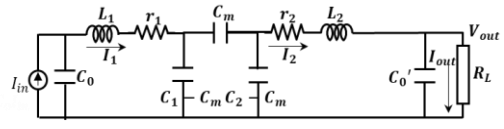

(a) CLC-CLC circuit in CPT connecting current source

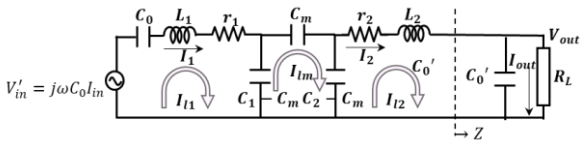

(b) Equivalent converted circuit

Fig. 9. CLC-CLC circuit in CPT.

Table 7. Efficiency in CPT.

Circuit	Efficiency
S-S	$\frac{k^2 Q_1 Q_2 r_2 R_L}{\{(1+k^2 Q_1 Q_2) r_2 + R_L\}(r_2 + R_L)}$
S-P	$\frac{k^2 Q_1 Q_2 [\{(1+Q_2^2) r_2 + R_L\}^2 + Q_2^2 R_L^2] r_2 R_L}{(1-k^2)^2 Q_2^2 r_2^2 \{(1+Q_2^2) r_2 + 2R_L\}^2 + \{(1+Q_2^2) r_2 + R_L\} R_L [(1-k^2)\{(1+Q_2^2) r_2 + R_L\} R_L + k^2 Q_1 Q_2 \{(r_2 + R_L)^2 + Q_2^2 r_2^2\}]}$
S-CLC	$\frac{k^2 Q_1 Q_2^3 r_2 R_L}{\{(1-k^2)^2 + k^2 Q_1 Q_2\}\{Q_2^2 r_2 (r_2 + R_L) + R_L^2\} + Q_2^2\{k^4 Q_2^2 r_2^2 + (1-k^2)^2 r_2 R_L + R_L^2\}}$
P-S	$\frac{k^2 Q_1 Q_2 r_2 R_L}{[\{(1-k^2)^2 + k^2 Q_1 Q_2\} r_2 + (1-k^2) R_L](r_2 + R_L) + k^4 Q_2^2 r_2^2}$
P-P	$\frac{k^2 Q_1 Q_2 [\{(1+Q_2^2) r_2 + R_L\}^2 + Q_2^2 R_L^2] r_2 R_L}{Q_2^2 \{Q_2^2 r_2^2 + (r_2 + R_L)^2 - (1-k^2) R_L^2\}^2 + \{(1+Q_2^2) r_2 + R_L\}[(1-k^2)^2 \{(1+Q_2^2) r_2 + R_L\} R_L + k^2 Q_1 Q_2 \{(r_2 + R_L)^2 + Q_2^2 r_2^2\}] R_L}$
P-CLC	$\frac{k^2 Q_1 Q_2^3 r_2 R_L}{\{(1-k^2)^2 + k^2 Q_1 Q_2\}\{Q_2^2 r_2 (r_2 + R_L) + R_L^2\} + Q_2^2\{k^4 Q_2^2 r_2^2 + (1-k^2)^2 r_2 R_L + R_L^2\}}$
CLC-S	$\frac{k^2 Q_1 Q_2 r_2 R_L}{[\{(1-k^2)^2 + k^2 Q_1 Q_2\} r_2 + (1-k^2) R_L](r_2 + R_L) + k^4 Q_2^2 r_2^2}$
CLC-P	$\frac{k^2 Q_1 Q_2 [\{(1+Q_2^2) r_2 + R_L\}^2 + Q_2^2 R_L^2] r_2 R_L}{Q_2^2 \{Q_2^2 r_2^2 + (r_2 + R_L)^2 - (1-k^2) R_L^2\}^2 + \{(1+Q_2^2) r_2 + R_L\}[(1-k^2)^2 \{(1+Q_2^2) r_2 + R_L\} R_L + k^2 Q_1 Q_2 \{(r_2 + R_L)^2 + Q_2^2 r_2^2\}] R_L}$
CLC-CLC	$\frac{k^2 Q_1 Q_2^3 r_2 R_L}{\{(1-k^2)^2 + k^2 Q_1 Q_2\}\{Q_2^2 r_2 (r_2 + R_L) + R_L^2\} + Q_2^2\{k^4 Q_2^2 r_2^2 + (1-k^2)^2 r_2 R_L + R_L^2\}}$

Table .8 Optimal Load in CPT.

Circuit	Optimal Load
S-S	$r_2\sqrt{1 + k^2 Q_1 Q_2}$
S-P	$Q_2 r_2 \sqrt{\frac{(1-k^2)(1+Q_2^2)}{1 - k^2 + k^2 Q_1 Q_2}}$
S-CLC	$Q_2 r_2 \sqrt{\frac{(1-k^2)^2 + k^4 Q_2^2 + k^2 Q_1 Q_2}{(1-k^2)^2 + Q_2^2 + k^2 Q_1 Q_2}}$
P-S	$r_2 \sqrt{\frac{(1-k^2)^2 + k^2 Q_1 Q_2 + k^4 Q_2^2}{(1-k^2)^2}}$
P-P	$Q_2 r_2 \sqrt{\frac{1 + Q_2^2}{(1-k^2)^2 + k^4 Q_2^2 + k^2 Q_1 Q_2}}$
P-CLC	$Q_2 r_2 \sqrt{\frac{(1-k^2)^2 + k^4 Q_2^2 + k^2 Q_1 Q_2}{(1-k^2)^2 + Q_2^2 + k^2 Q_1 Q_2}}$
CLC-S	$\frac{r_2}{1-k^2}\sqrt{(1-k^2)^2 + k^4 Q_2^2 + k^2 Q_1 Q_2}$
CLC-P	$Q_2 r_2 \sqrt{\frac{1 + Q_2^2}{(1-k^2)^2 + k^4 Q_2^2 + k^2 Q_1 Q_2}}$
CLC-CLC	$Q_2 r_2 \sqrt{\frac{(1-k^2)^2 + k^4 Q_2^2 + k^2 Q_1 Q_2}{(1-k^2)^2 + Q_2^2 + k^2 Q_1 Q_2}}$

5. Output Power

5.1 Output Power in IPT The F parameter of LCL-LCL circuit in IPT can be expressed as in equation (36). Here, F parameters in equation (36) show the form in which the compensation conditions presented in equation (11) are applied.

$$\begin{cases} A = \frac{j\omega}{L_m}\{C_2 r_2 (L_0 + C_1 r_0 r_1) + \omega^2 L_m^2 C_1 C_2 r_0\} \\ B = \frac{j\omega}{L_m}\{(L_0 + C_1 r_0 r_1)(L_0' + C_2 r_2 r_0') + \omega^2 L_m^2 C_1 C_2 r_0 r_0'\} \\ C = \frac{j\omega}{L_m}(r_1 r_2 + \omega^2 L_m^2) C_1 C_2 \\ D = \frac{j\omega}{L_m}\{C_1 r_1 (L_0' + C_2 r_2 r_0') + \omega^2 L_m^2 C_1 C_2 r_0'\} \end{cases} \cdots\cdots (36)$$

The relationship between V_{out} and I_{out} is equation (37). From equation (7), (36) and (37), V_{in} can be expressed as in equation (38). In addition, the output power when using a voltage source P_{out_Vin} in LCL-LCL can be obtained from equation (39). Therefore, P_{out_Vin} in LCL-LCL circuit is as in equation (40).

$$V_{out} = R_L I_{out} \cdots\cdots (37)$$

$$V_{in} = \frac{j\omega I_{out}}{L_m}[(L_0 + C_1 r_0 r_1)\{L_0' + C_2 r_2 (r_0' + R_L)\} + \omega^2 L_m^2 C_1 C_2 (r_0' + R_L)] \cdots\cdots (38)$$

$$P_{out} = R_L |I_{out}|^2 \cdots\cdots (39)$$

$$P_{out\_Vin}^{LCL-LCL} = \frac{k^2 Q_1^3 Q_2^3 r_2 R_L |V_{in}|^2}{r_1[\{(1+Q_1^2)(1+Q_2^2) + k^2 Q_1 Q_2) r_2 + (1+Q_1^2+k^2 Q_1 Q_2) R_L\}^2]} \cdots\cdots (40)$$

Similarly, for the other circuits is calculated as shown in Table 9.

Also, input current I_{in} is expressed in equation (41), so from equation (42), the output power circuit when using a current source P_{out_Iin} in LCL-LCL is obtained as in equation (43).

$$I_{in} = \frac{j\omega V_{out}}{L_m R_L}\{(r_1 r_2 + \omega^2 L_m^2) C_1 C_2 (r_0' + R_L) + L_0' C_1 r_1\} \cdots\cdots (41)$$

$$P_{out} = |V_{out}|^2 / R_L \cdots\cdots (42)$$

$$P_{out\_Iin}^{LCL-LCL} = \frac{k^2 Q_1^3 Q_2^3 r_1 r_2 R_L |I_{in}|^2}{\{(1+Q_2^2+k^2 Q_1 Q_2) r_2 + (1+k^2 Q_1 Q_2) R_L\}^2} \cdots\cdots (43)$$

The results of the output power for the other circuits in the same way are shown in Table 9 and 10.

Table 9. Output power connecting voltage source in IPT.

Circuit	Output power connecting current source
S-S	$\frac{k^2 Q_1 Q_2 r_2 R_L \lvert V_{in}\rvert^2}{r_1\{(1+k^2 Q_1 Q_2) r_2 + R_L\}^2}$
S-P	$\frac{k^2 Q_1 Q_2^3 r_2 R_L \lvert V_{in}\rvert^2}{r_1[\{Q_2^2 r_2 + R_L + k^2 Q_1 Q_2 (r_2 + R_L)\}^2 + (Q_2 r_2 - k^2 Q_1 R_L)^2]}$
S-LCL	$\frac{k^2 Q_1 Q_2^3 r_2 R_L \lvert V_{in}\rvert^2}{r_1\{(1+Q_2^2+k^2 Q_1 Q_2) r_2 + (1+k^2 Q_1 Q_2) R_L\}^2}$
P-S	$\frac{k^2 Q_1 Q_2 r_2 R_L \lvert V_{in}\rvert^2}{r_1[(r_2 + R_L)^2 + \{(Q_1 + k^2 Q_2) r_2 + Q_1 R_L\}^2]}$
P-P	$\frac{k^2 (1-k^2)^2 Q_1 Q_2^3 r_2 R_L \lvert V_{in}\rvert^2}{r_1\left(\begin{matrix}[(1-k^2)\{1-(1-k^2) Q_1 Q_2\} Q_2 r_2 - \{(1-k^2) Q_1 + k^2 Q_2\} R_L]^2 \\ +[(1-k^2)(Q_1 + Q_2) Q_2 r_2 + \{1-k^2(1+k^2 Q_1 Q_2)\} R_L]^2\end{matrix}\right)}$
P-LCL	$\frac{k^2 Q_1 Q_2^3 r_2 R_L \lvert V_{in}\rvert^2}{r_1[\{(1+Q_2^2) r_2 + (1+k^2 Q_1 Q_2) R_L\}^2 + Q_1^2\{(1+Q_2^2) r_2 + R_L\}^2]}$
LCL-S	$\frac{k^2 Q_1^3 Q_2 r_2 R_L \lvert V_{in}\rvert^2}{r_1\{(1+Q_1^2+k^2 Q_1 Q_2) r_2 + (1+Q_1^2) R_L\}^2}$
LCL-P	$\frac{k^2 Q_1^3 Q_2^3 r_2 R_L \lvert V_{in}\rvert^2}{r_1[(1+Q_1^2+k^2 Q_1 Q_2)^2 Q_2^2 r_2^2 + \{(1+Q_1^2) Q_2^2 r_2 + (1+Q_1^2+k^2 Q_1 Q_2) R_L\}^2]}$
LCL-LCL	$\frac{k^2 Q_1^3 Q_2^3 r_2 R_L \lvert V_{in}\rvert^2}{r_1[\{(1+Q_1^2)(1+Q_2^2) + k^2 Q_1 Q_2) r_2 + (1+Q_1^2+k^2 Q_1 Q_2) R_L\}^2]}$

Table 10. Output power connecting current source in IPT.

Circuit	Output power connecting voltage source
S-S	$\frac{k^2 Q_1 Q_2 r_1 r_2 R_L \lvert I_{in}\rvert^2}{(r_2 + R_L)^2}$
S-P	$\frac{k^2 Q_1 Q_2^3 r_1 r_2 R_L \lvert I_{in}\rvert^2}{r_2^2 + (Q_2^2 r_2 + R_L)^2}$
S-LCL	$\frac{k^2 Q_1 Q_2^3 r_1 r_2 R_L \lvert I_{in}\rvert^2}{\{(1+Q_2^2) r_2 + R_L\}^2}$
P-S	$\frac{k^2 Q_1^3 Q_2 r_1 r_2 R_L \lvert I_{in}\rvert^2}{\{(1+k^2 Q_1 Q_2) r_2 + R_L\}^2 + k^4 Q_2^2 r_2^2}$
P-P	$\frac{k^2 (1-k^2) Q_1^3 Q_2^3 r_1 r_2 R_L \lvert I_{in}\rvert^2}{[(1-k^2)(k^2 Q_1 + Q_2) Q_2 r_2 + \{1 + k^2 (1-k^2) Q_1 Q_2\} R_L]^2 + \{(1-k^2) Q_2 r_2 - k^2 (Q_1 + Q_2) R_L\}^2}$
P-LCL	$\frac{k^2 Q_1^3 Q_2^3 r_1^3 r_2 R_L \lvert I_{in}\rvert^2}{\{(1+Q_2^2+k^2 Q_1 Q_2) r_1 r_2 + (1+k^2 Q_1 Q_2) r_1 R_L + r_2^2\}^2}$
LCL-S	$\frac{k^2 Q_1^3 Q_2 r_1 r_2 R_L \lvert I_{in}\rvert^2}{\{(1+k^2 Q_1 Q_2) r_2 + R_L\}^2}$
LCL-P	$\frac{k^2 Q_1^3 Q_2^3 r_1 r_2 R_L \lvert I_{in}\rvert^2}{(1+k^2 Q_1 Q_2)^2 Q_2^2 r_2^2 + \{Q_2^2 r_2 + (1+k^2 Q_1 Q_2) R_L\}^2}$
LCL-LCL	$\frac{k^2 Q_1^3 Q_2^3 r_1 r_2 R_L \lvert I_{in}\rvert^2}{\{(1+Q_2^2+k^2 Q_1 Q_2) r_2 + (1+k^2 Q_1 Q_2) R_L\}^2}$

5.2 Output Power in CPT The F parameter of CLC-CLC circuit in CPT can be expressed as in equation (44).

$$\begin{cases} A = \frac{j\omega}{C_m}\{\omega^2 L_1 C_0' C_m^2 r_1 + C_1 C_2 r_1 (1 + \omega C_0' r_2) - j\omega C_0' C_m^2 r_1 r_2\} \\ B = \frac{j\omega}{C_m}\{(\omega^2 L_1 L_2 - r_1 r_2) C_m^2 + C_1 C_2 r_1 r_2 - j\omega (L_1 r_2 + L_2 r_1)\} \\ C = \frac{j\omega}{C_m}\{\omega^2 C_0 C_0' C_m^2 r_1 r_2 + j\omega C_0 C_2 (1 + \omega C_1 r_2)(1 + \omega C_0' r_2)\} \\ D = \frac{j\omega}{C_m}\{\omega^2 L_2 C_0 C_m^2 r_1 + C_0 C_2 r_2 - j\omega L_2 C_0 C_m^2 r_1 r_2\} \end{cases} (44)$$

In the same way as IPT, the output power when a voltage source is connected can be obtained as in equation (45).

$$P_{out\_Vin}^{CLC-CLC} = \frac{k^2 Q_1 Q_2^3 r_2 R_L |V_{in}|^2}{r_1\left[\begin{matrix}[(1-k^2+k^2 Q_1 Q_2) Q_2 r_2 + (k^2 Q_1 + Q_2) R_L]^2 \\ +\{k^2 (Q_1 + Q_2) Q_2 r_2 - (1-k^2) R_L\}^2\end{matrix}\right]} \cdots\cdots (45)$$

Table 11. Output power connecting voltage source in CPT.

Circuit	Output power connecting voltage source
S-S	$\frac{k^2 Q_1 Q_2 r_1 r_2 R_L \lvert V_{in}\rvert^2}{r_1\{(1+k^2 Q_1 Q_2) r_2 + R_L\}}$
S-P	$\frac{k^2 (1-k^2) Q_1 Q_2 (1+Q_2^2)^2 r_2 R_L \lvert V_{in}\rvert^2}{r_1\left[k^4 (1+Q_2^2)^2 R_L^2 + \{(1+Q_2^2)((1-k^2) Q_2 r_2 + k^2 Q_1 R_L) + (1-k^2) Q_2 R_L\}^2\right]}$
S-CLC	$\frac{k^2 Q_1 Q_2^3 r_2 R_L \lvert V_{in}\rvert^2}{r_1\left[\begin{matrix}[(1-k^2+k^2 Q_1 Q_2) Q_2 r_2 + (k^2 Q_1 + Q_2) R_L]^2 \\ +\{k^2 (Q_1 + Q_2) Q_2 r_2 - (1-k^2) R_L\}^2\end{matrix}\right]}$
P-S	$\frac{k^2 Q_2 r_2 R_L \lvert V_{in}\rvert^2}{(1-k^2) Q_1 r_1 (r_2 + R_L)^2}$
P-P	$\frac{k^2 (1+Q_2^2)^2 Q_2 r_2 R_L \lvert V_{in}\rvert^2}{Q_1 r_1[\{(1+Q_2^2) Q_2 r_2 + R_L\}^2 + R_L^2]}$
P-CLC	$\frac{k^2 Q_2^3 r_2 R_L \lvert V_{in}\rvert^2}{Q_1 r_1\{Q_2^2 (r_2 + R_L)^2 + R_L^2\}}$
CLC-S	$\frac{k^2 Q_1 Q_2 r_2 R_L \lvert V_{in}\rvert^2}{r_1[\{(1-k^2+k^2 Q_1 Q_2) r_2 + (1-k^2) R_L\}^2 + k^4\{(Q_1 + Q_2) r_2 + Q_1 R_L\}^2]}$
CLC-P	$\frac{k^2 Q_1 Q_2 (1+Q_2^2)^2 r_2 R_L \lvert V_{in}\rvert^2}{r_1((1-k^2(1+Q_2^2))^2 R_L^2 + [(1+Q_2^2) Q_2 r_2 + \{k^2 Q_1 + (1+k^2 Q_1 Q_2) Q_2\} R_L]^2)}$
CLC-CLC	$\frac{k^2 Q_1 Q_2^3 r_2 R_L \lvert V_{in}\rvert^2}{r_1[\{(1-k^2+k^2 Q_1 Q_2) Q_2 r_2 + (k^2 Q_1 + Q_2) R_L\}^2 + \{k^2 (Q_1 + Q_2) Q_2 r_2 - (1-k^2) R_L\}^2]}$

Table 12. Output power connecting current source in CPT.

Circuit	Output power connecting current source
S-S	$\frac{k^2Q_1Q_2r_1r_2R_L\|I_{in}\|^2}{(r_2+R_L)^2}$
S-P	$\frac{k^2Q_1Q_2(1+Q_2^2)^2r_1r_2R_L\|I_{in}\|^2}{(1-k^2)[Q_2^2\{(1+Q_2^2)r_2+R_L\}^2+R_L^2]}$
S-CLC	$\frac{k^2Q_1Q_2^3r_1r_2R_L\|I_{in}\|^2}{\{k^2Q_2^2r_2-(1-k^2)R_L\}^2+Q_2^2\{(1-k^2)r_2+R_L\}^2}$
P-S	$\frac{k^2(1-k^2)^2(1+Q_1^2)^2Q_1Q_2r_1r_2R_L\|I_{in}\|^2}{[\{(1-k^2+k^2Q_1Q_2)Q_1+k^2Q_2\}r_2+(1-k^2)Q_1R_L]^2+(1-k^2)^2(r_2+R_L)^2}$
P-P	$\frac{k^2(1+Q_1^2)^2(1+Q_2^2)^2Q_1Q_2r_1r_2R_L\|I_{in}\|^2}{[(1+Q_2^2)Q_1Q_2r_2+\{k^2(1+Q_1^2)(1+Q_2^2)+Q_1Q_2-1\}R_L]^2+\{(1+Q_2^2)Q_2r_2+(Q_1+Q_2)R_L\}^2}$
P-CLC	$\frac{k^2Q_1Q_2^3(1+Q_1^2)^2r_1r_2R_L\|I_{in}\|^2}{\{(1+k^2Q_1Q_2)Q_1Q_2r_2-\{1-k^2(1+Q_1^2)+Q_1Q_2\}R_L\}^2+Q_2^2\{(1-k^2-k^2Q_1Q_2)r_2+Q_1R_L\}^2}$
CLC-S	$\frac{k^2Q_1^3Q_2r_1r_2R_L\|I_{in}\|^2}{(1-k^2)(r_2+R_L)^2+\{(Q_1+k^2Q_2)r_2+Q_1R_L\}^2}$
CLC-P	$\frac{k^2Q_1^3Q_2(1+Q_2^2)^2r_1r_2R_L\|I_{in}\|^2}{\{Q_2(1+Q_2^2)r_2+(Q_1+Q_2)R_L\}^2+\{Q_1Q_2(1+Q_2^2)r_2-(1-k^2-Q_1Q_2-k^2Q_1Q_2)R_L\}^2}$
CLC-CLC	$\frac{k^2Q_1^3Q_2^3r_1r_2R_L\|I_{in}\|^2}{\{(Q_1+k^2Q_2)Q_2r_2-(1-k^2-Q_1Q_2)R_L\}^2+(Q_1+Q_2)^2R_L^2}$

The output power when a current source is connected in CLC-CLC is shown in equation (42).

$$P_{out\_Iin}^{CLC-CLC}=\frac{k^2Q_1^3Q_2^3r_1r_2R_L|I_{in}|^2}{\{(Q_1+k^2Q_2)Q_2r_2-(1-k^2-Q_1Q_2)R_L\}^2+(Q_1+Q_2)^2R_L^2} \cdots\cdots (46)$$

For the other circuits, the output power when a current source is connected is shown in Table 12.

6. Comparison with Simulation

In order to verify that the respective equations for the transmission characteristics obtained in Chapters 3-5 are correct, a comparison with the simulation values was carried out. The simulation is an electromagnetic simulation using the moment method, the coupler used in the simulation is shown in Fig. 10 and the parameters in Table 13. For a fair comparison, Q values, coupling coefficients$k$ and power supply performance are unified. In addition, the coupling coefficients k , Q values are configured so that the coupler area is close to the values while the values are aligned. Furthermore, in order to match k and Q in IPT and CPT, an external capacitor is used in addition to the transmission capacitor in CPT.

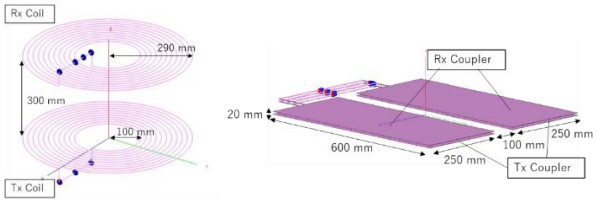

(a) Transmission coils (b) Transmission plates

Fig. 10. Transmission coupler.

Table 13. Parameters of simulation.

	Symbol	Value	
Voltage Source	V_{in}	30 V	
Current Source	I_{in}	1 A	
Coupling Factor	k	0.11	
Q value	Q_0, Q_1, Q_2, Q_0'	231.02	
		IPT	CPT
Resonant Frequency	f	85 kHz	450 kHz
Inductance	L_0, L_1, L_2, L_0'	51.85 μH	independent on k 138.05 μH depend on k 139.76 μH
Internal Resistance	r_0, r_1, r_2, r_0'	0.12 ohm	independent on k 1.69 ohm depend on k 1.71 ohm
Capacitance	C_0, C_1, C_2, C_0'	independent on k 67.62 pF depend on k 68.41 nF	906.08 nF

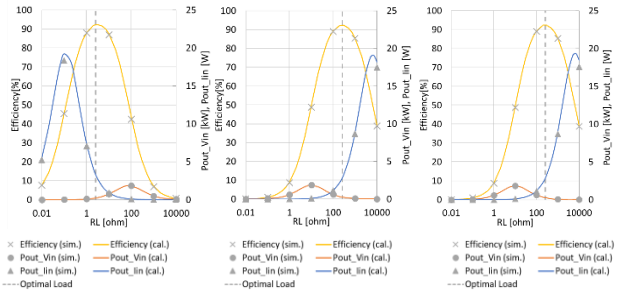

(a)S-S (b)S-P (c)S-LCL

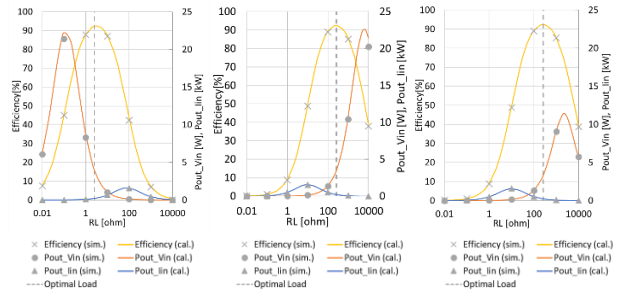

(d)P-S (e)P-P (f)P-LCL

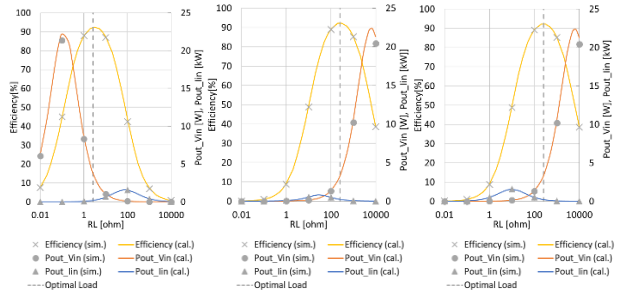

(g)LCL-S (h)LCL-P (i)LCL-LCL

Fig. 11. Comparison of simulation and calculation in IPT.

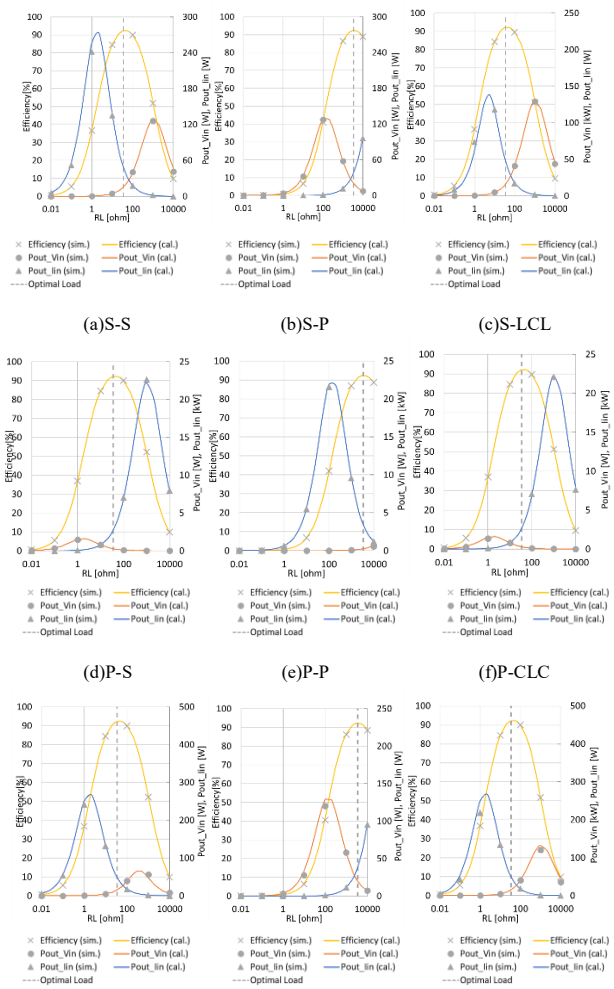

(a)S-S (b)S-P (c)S-LCL

(d)P-S (e)P-P (f)P-CLC

(g)CLC-S (h)CLC-P (i)CLC-CLC

Fig. 12. Comparison of simulation and calculation in CPT.

The results of the calculation and simulation of efficiency and output power are shown in Fig. 11, 12. Fig. 11, 12 show that the equations derived in Chapter 3-5 are correct, as the calculation and simulation results are in agreement.

7. Comparison of Transmission Characteristics

In this chapter, the parameters of the unification condition used in the simulation, as presented in Table 13, are substituted into the respective equations of the transmission characteristics derived in Chapters 3-5 to compare the transmission characteristics.

7.1 Optimal Load The optimal load for each circuit of IPT and the optimal load for each circuit of CPT are as shown in Fig. 13. The optimal load in IPT has a small value when the receiver side is S and a large value when the receiver side is P and LCL. In CPT, it has a small value when the receiver side is S and LCL and a large value when the receiver side is P.

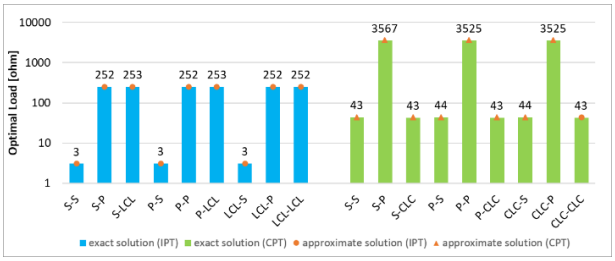

Fig. 13. Optimal Load.

Here, using the approximation of equation (47) to the exact equation of optimal load derived in Chapter 4, the smaller optimal load R_{Lopt}^{Small} and the larger optimal load R_{Lopt}^{Large} can be expressed as equations (48), (49) in common with IPT and CPT.

$$Q_1 = Q_2 = Q, r_1 = r_2 = r, 1 + Q^2 \approx Q^2, 1 + k^2 \approx 1 \cdots (47)$$

$$R_{Lopt}^{Small} = r\sqrt{1 + k^2 Q^2} \cdots (48)$$

$$R_{Lopt}^{Large} = \frac{Q^2 r}{\sqrt{1+k^2 Q^2}} \cdots (49)$$

Furthermore, using the approximation in equation (50) R_{Lopt}^{Small} and R_{Lopt}^{Large} the relationship as in equation (51) can be obtained.

$$1 + k^2 Q^2 \approx k^2 Q^2 \cdots (50)$$

$$R_{Lopt}^{Small} : R_{Lopt}^{Large} = k^2 : 1 \cdots (51)$$

Therefore, when the approximation conditions in equations (47) and (50) can be applied, the value of R_{Lopt}^{Large} is $1/k^2$ times as large as the value of R_{Lopt}^{Small}.

From the above, higher efficiency can be obtained by selecting the receiver circuit according to the value of the load.

7.2 Maximum Efficiency The results for the maximum efficiency at optimal load are shown in Fig. 14, which shows that the efficiency is similar for all circuits regardless of IPT and CPT

Here, the maximum efficiency can also be calculated by applying the approximation in (47) to the exact equation derived in Chapter 4 and applying the optimal load in equation (48) or (49). The maximum efficiency in all circuits for both IPT and CPT can be expressed as in equation (52) by approximation.

$$\eta_{max}^{all\ circuits} = \frac{k^2 Q^2}{\left(1+\sqrt{1+k^2 Q^2}\right)^2} \cdots (52)$$

Therefore, if the approximation in equation (47) is applied, at optimal load, the maximum efficiency is common regardless of the method or circuit.

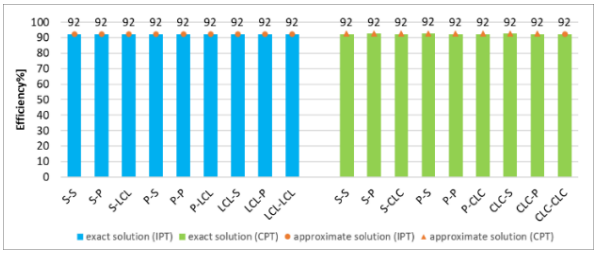

Fig. 14. Maximum Efficiency

7.3 Output Power connecting Voltage Source The results obtained for the output power of the voltage source at the optimal load are shown in Fig. 15. From Fig. 15, it can be seen that higher power is obtained when the transmitter side is S in IPT and when the transmitter side is S or CLC in CPT.

Here, the approximation in equation (47) and the optimal load in equation (48) or (49) are used in the exact equation for the output power when the voltage source is connected, as derived in Chapter 5. The resulting output power of the higher $P_{out\_Vin}^{High}$ and the lower output power $P_{out\_Vin}^{Low}$ can be expressed as in equations (47) and (48) in common with IPT and CPT.

$$P_{out\_Vin}^{High} = \frac{k^2Q^2|V_{in}|^2}{r\sqrt{1+k^2Q^2}\left(1+\sqrt{1+k^2Q^2}\right)^2} \quad \cdots\cdots (53)$$

$$P_{out\_Vin}^{Low} = \frac{k^2\sqrt{1+k^2Q^2}|V_{in}|^2}{r\left(1+\sqrt{1+k^2Q^2}\right)^2} \quad \cdots\cdots (54)$$

Furthermore, using equation (50), the relationship shown in equation (55) can be obtained. The value of $P_{out\_Vin}^{High}$ is $1/k^2$ times as high as the value of $P_{out\_Vin}^{Low}$.

$$P_{out\_Vin}^{High} : P_{out\_Vin}^{Low} = 1 : k^2 \quad \cdots\cdots (55)$$

Therefore, when using a voltage source, large power can be obtained by using S on the transmission side in IPT and S or CLC on the transmitter side in CPT.

7.4 Output Power connecting Current Source The results obtained for the output power when the current source is connected at the optimal load are shown in Fig. 16. From Fig. 16, it can be seen that IPT has a larger value when the transmitter side is a P or LCL circuit and CPT has a larger value when the transmitter side is a P circuit.

Here, the approximation of equation (47) and the optimal load of equation (48) or (49) are used in the exact equation for the output power of the current source derived in Chapter 5. The resulting output power of the higher $P_{out\_Iin}^{High}$ and the lower output power $P_{out\_Iin}^{Low}$ can be expressed as equations (56) and (57) in common with IPT and CPT.

$$P_{out\_Iin}^{High} = \frac{k^2Q^4r|I_{in}|^2}{\sqrt{1+k^2Q^2}\left(1+\sqrt{1+k^2Q^2}\right)^2} \quad \cdots\cdots (56)$$

$$P_{out\_Iin}^{Low} = \frac{k^2Q^2r\sqrt{1+k^2Q^2}|I_{in}|^2}{\left(1+\sqrt{1+k^2Q^2}\right)^2} \quad \cdots\cdots (57)$$

In addition, under the approximate conditions of equation (50), their relation can be expressed by equation (58). The value of $P_{out\_Vin}^{High}$ is $1/k^2$ times as high as the value of $P_{out\_Vin}^{Low}$.

$$P_{out\_Iin}^{High} : P_{out\_Iin}^{Low} = 1 : k^2 \quad \cdots\cdots (58)$$

Therefore, when using a current source, to obtain higher power, it is suitable to use P or LCL on the transmitter side in IPT and P on the transmitter side in CPT.

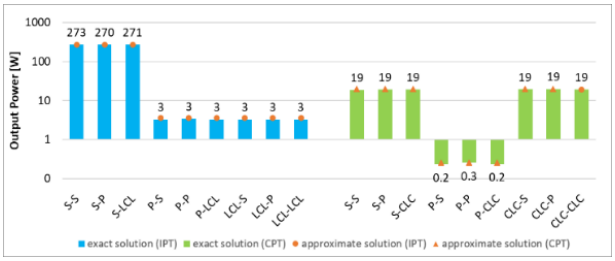

Fig. 15. Output power connecting voltage source.

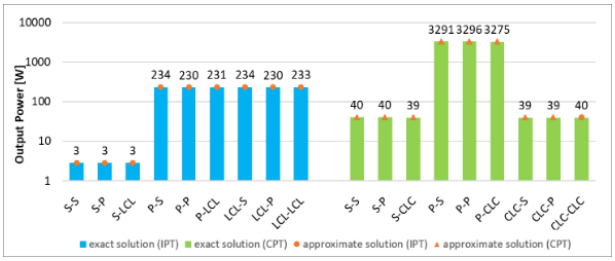

Fig. 16. Output power connecting current source.

7.5 Summary of Transmission Characteristics The transmission characteristics of the circuits obtained from the above are summarised in Table 14. Here, The results are summarised here when the power supply is as the voltage source, as it is commonly used.

As a result of the evaluation of the good points using ✓ marks, it can be concluded that S-S, S-LCL, LCL-S, LCL-P and LCL-LCL are superior in IPT and S-CLC, P-P, P-CLC, CLC-P and CLC-CLC are superior in CPT.

Furthermore, under the approximate conditions as in equation (47), (50), the equations common to IPT and CPT were obtained for all efficiency, optimum load, and output power.

Table 14. Summary of Transmission Characteristics.

		$k=0$ Characteristic	Compensation Condition	CC/CV Characteristic	Optimal Load	Efficiency	Output Power	Number of ✓
IPT ✓long distance ✓low dielectric impact	S-S	Large Current	✓Independent on k	✓CC	Small	✓High	✓High	✓4
	S-P	Large Current	Depend on k	✓CV	Large	✓High	✓High	3
	S-LCL	Large Current	✓Independent on k	✓CV	Large	✓High	✓High	✓4
	P-S	✓Small Current	Depend on k	✓CV	Small	✓High	Low	3
	P-P	✓Small Current	Depend on k	✓CC	Large	✓High	Low	3
	P-LCL	✓Small Current	✓Independent on k	None	Large	✓High	Low	3
	LCL-S	✓Small Current	✓Independent on k	✓CV	Small	✓High	Low	✓4
	LCL-P	✓Small Current	✓Independent on k	✓CC	Large	✓High	Low	✓4
	LCL-LCL	✓Small Current	✓Independent on k	✓CC	Large	✓High	Low	✓4
CPT ✓low cost ✓low metal impact ✓light weight	S-S	Large Current	Depend on k	✓CC	Small	✓High	✓High	3
	S-P	Large Current	Depend on k	✓CV	Large	✓High	✓High	3
	S-CLC	Large Current	✓Independent on k	✓CC	Small	✓High	✓High	✓4
	P-S	✓Small Current	Depend on k	✓CV	Small	✓High	Low	3
	P-P	✓Small Current	✓Independent on k	✓CC	Large	✓High	Low	✓4
	P-CLC	✓Small Current	✓Independent on k	✓CV	Small	✓High	Low	✓4
	CLC-S	Large Current	✓Independent on k	None	Small	✓High	✓High	3
	CLC-P	Large Current	✓Independent on k	✓CV	Large	✓High	✓High	✓4
	CLC-CLC	Large Current	✓Independent on k	✓CC	Small	✓High	✓High	✓4

8. Qualitative Study of Output Power

From Chapter 7, it was found that the magnitude of the output power depends on the transmitter side circuit. This chapter provides the qualitative study for output power.

8.1 Impedance on Receiver Side The impedance of the receiver side Z_{Rx}, as shown in Fig. 17, is important for a qualitative study. The equation of the impedance on the receiver side of each circuit at the optimal load is shown in Table 15.

Applying the approximation of equation (47) to the equations given in Table 15. allows the receiver side impedance to be expressed in a common for each transmission method, as in equations (59) and (60).

$$Z_{Rx}^{IPT} = r\left(1+\sqrt{1+k^2Q^2}\right) \quad \cdots\cdots (59)$$

$$Z_{Rx}^{CPT} = \frac{Q^2 r}{1+\sqrt{1+k^2Q^2}} \quad \cdots\cdots (60)$$

Furthermore, from the gyrator characteristics of the coupler section, the impedance in the front of the coupler Z_m^{IPT}, Z_m^{CPT} are as in equations (61) and (62).

$$Z_m^{IPT} = \frac{\omega^2 L_m^2}{Z_{Rx}} = \frac{k^2Q^2r^2}{Z_{Rx}} = \frac{k^2Q^2r}{1+\sqrt{1+k^2Q^2}} \quad \cdots\cdots (61)$$

$$Z_m^{CPT} = \frac{1}{\omega^2 C_m^2 Z_{Rx}} = \frac{Q^2r^2}{k^2 Z_{Rx}} = \frac{r\left(1+\sqrt{1+k^2Q^2}\right)}{k^2} \quad \cdots\cdots (62)$$

Therefore, the output power depends on the transmitter side configuration, as shown in Chapter 7 - 3 and 4, because the impedance on the receiver side is common for each transmission method at the optimal load.

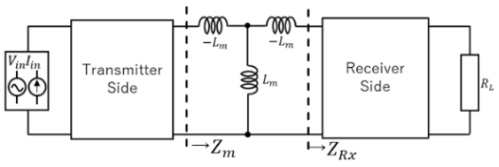

(a)IPT

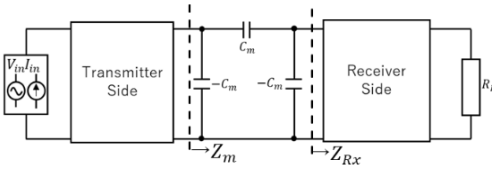

(b)CPT

Fig. 17. Impedance of each part.

Table 15. Impedance on receiver side.

Method	Circuit	Receiver impedance
IPT	S	$r_2 + R_L$
	P	$r_2\sqrt{\left(1+\frac{Q_2^2 r_2 R_L}{Q_2^2 r_2^2 + R_L^2}\right)^2 + \left(\frac{Q_2^3 r_2^2}{Q_2^2 r_2^2 + R_L^2}\right)^2}$
	LCL	$r_2 + \frac{Q_2^2 r_2^2}{r_2 + R_L}$
CPT	S	$\frac{Q_2 r_2}{r_2 + R_L}\sqrt{Q_2^2 r_2^2 + (r_2 + R_L)^2}$
	P	$\frac{Q_2 r_2 R_L \sqrt{Q_2^2\{(1+Q_2^2)r_2 + R_L\}^2 + R_L^2}}{Q_2^2 r_2^2 + (Q_2^2 r_2 + R_L)^2}$
	LCL	$\frac{Q_2 r_2 \sqrt{Q_2^6 r_2^2 (2r_2 + R_L)^2 + \{Q_2^2(r_2^2 + r_2 R_L + R_L^2) + R_L^2\}^2}}{Q_2^2(r_2 + R_L)^2 + R_L^2}$

8.2 CC/CV Characteristic on Transmitter Side and Output Power

The relationship between CC/CV characteristic of the transmitter side and the magnitude of the output power is shown in Table 14.

From Table 16, it can be seen that in the case of IPT the output power is higher when CC/CV characteristic on the transmitter has CV characteristic. Furthermore, in the case of CPT the output power is higher when CC/CV characteristic on the transmitter has CC characteristic.

Here, Z_m^{IPT}, and Z_m^{CPT} ratio can be expressed in equation (63) using equation (50).

$$Z_m^{IPT} : Z_m^{CPT} = k^2 : 1 \quad \cdots\cdots (63)$$

Therefore, The value of Z_m^{CPT} is $1/k^2$ times as large as the value of Z_m^{IPT}.

From the above, it can be said that IPT can obtain a high power when the transmission side has CV characteristic because the impedance in the front of the coupler Z_m^{IPT} is small, and CPT can obtain a high power when the transmission side has CC characteristic because the impedance in the front of the coupler Z_m^{CPT} is large.

Table 16. CC/CV characteristic on transmitter side and Output Power

Method	circuit	Power supply	CC/CV characteristic	Output power
IPT	S	voltage source	**CV**	**High**
		current source	CC	Low
	P	voltage source	None	Low
		current source	**CV**	**High**
	LCL	voltage source	CC	Low
		current source	**CV**	**High**
CPT	S	voltage source	**CC**	**High**
		current source	None	Low
	P	voltage source	CV	Low
		current source	**CC**	**High**
	CLC	voltage source	**CC**	**High**
		current source	CV	Low

9. Comparison with Experiment

The Experiment were carried out to verify the transmission characteristics in actual conditions. The parameters used are shown in Table 14 and 18. A vector network analyser (VNA) was used for the measurements . The experimental environments are shown in Fig. 18. Here, in order to match k and Q in IPT and CPT, an external capacitor is used in addition to the transmission capacitor in CPT.

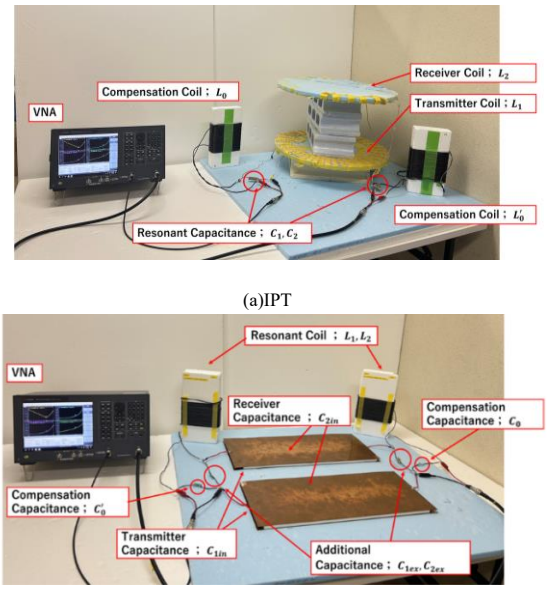

(a)IPT

(b)CPT

Fig. 18. Experiment environment.

Table 17. Parameters of experiment in IPT

	symbol	value
Voltage Source	V_{in}	10
Coupling Factor	k	0.10
Resonant Frequency	f	85 kHz
Transmission Inductance	L_1, L_2	96.73 μH, 97.09μH
Internal Resistance	r_1, r_2	0.36 ohm, 0.46 ohm
Compensation Inductance	L_0, L_0'	98.76μH, 98.81μH
Internal Resistance	r_0, r_0'	0.38 ohm, 0.40 ohm
Resonant Capacitance	C_1, C_2	35.95 pF, 35.14 pF
Q value	Q_1, Q_2	142.39, 113.93

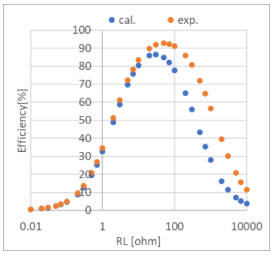

(a)Efficiency

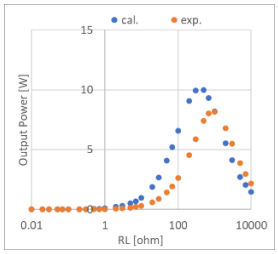

(b)Output power

Fig. 19. Comparison of experiment and calculation for LCL-LCL in IPT.

Table 18. Parameters of experiment in CPT

	symbol	value
Voltage Source	V_{in}	10
Coupling Factor	k	0.08
Resonant Frequency	f	450 kHz
Transmission Capacitance	C_1, C_2	889.04 pF, 887.64 pF
Compensation Capacitance	C_0, C_0'	915.49 pF, 907.81 pF
Resonant Inductance	L_1, L_2	139.19 μH, 134.35 μH
Internal Resistance	r_1, r_2	2.44 ohm, 2.03 ohm
Q value	Q_1, Q_2	161.12, 186.85

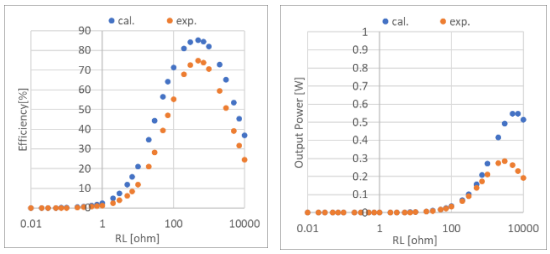

(a)Efficiency (b)Output power

Fig. 20. Comparison of experiment and calculation for CLC-CLC in CPT.

The calculated and experimental results obtained for efficiency and output power with varying loads are shown in Figs. 19 and 20. The results for LCL-LCL circuit in IPT and CLC-CLC circuit in CPT are shown here as representative. It can be seen that the experimental and calculated results are in general agreement. Therefore, it can be shown that the transmission characteristics presented in this paper are same even in actual environment.

10. Conclusion

In this paper, circuits consisting of series, parallel and LCL/CLC resonance are compared in a general and systematic. In terms of compensation condition and CC/CV characteristic, S-S and LCL-LCL in IPT and P-P and CLC-CLC in CPT can be said to correspond to each other in that the compensation conditions are independent of the coupling coefficient and have gyrator characteristic. The optimal load for both IPT and CPT varies depending on the receiver side, so it is necessary to select the appropriate circuit on the receiver side according to the value of the load. As for the maximum efficiency, it is clear that it does not depend on the transmission method or circuit. In terms of output power, common to IPT and CPT, the magnitude of the output power varies with the transmitter side. When using a voltage source, IPT are superior to S on the transmitter side and CPT are superior to S or CLC on the transmitter side. When using a current source, IPT can obtain higher power by selecting P or LCL for the transmitter side and P for the transmitter side for CPT. Furthermore, by using the approximate conditional equation, a qualitative study has found that IPT can obtain high power when the transmitter side has CC characteristic and CPT when the transmitter side has the CV characteristic. From the above, it can be concluded that S-S, S-LCL, LCL-S, LCL-P and LCL-LCL are superior in IPT and S-CLC, P-P, P-CLC, CLC-P and CLC-CLC in CPT. As the optimal load values vary from large to small, a suitable circuit can be selected from the above according to the optimal load

References

(1) M. P. Theodoridis, "Effective Capacitive Power Transfer," in IEEE Transactions on Power Electronics, vol. 27, no. 12, pp. 4906-4913, Dec. 2012.

(2) "Goodbye wires! Franklin Hadley;“ MIT team experimentally demonstrates wireless power transfer, potentially useful for powering laptops, cell phones without cords” MIT News, 2007.," 2020.

(3) Y. H. Sohn, B. H. Choi, E. S. Lee, G. C. Lim, G. -H. Cho and C. T. Rim, "General Unified Analyses of Two-Capacitor Inductive Power Transfer Systems: Equivalence of Current-Source SS and SP Compensations," in IEEE Transactions on Power Electronics, vol. 30, no. 11, pp. 6030-6045, Nov. 2015

(4) S. Kuroda and T. Imura, "Resonant circuit topology Comparison and CC / CV Characteristic Evaluation Considering the Difference in Power Supply in Capacitive Wireless Power Transfer circuits," IECON 2021 – 47th Annual Conference of the IEEE Industrial Electronics Society, Toronto, ON, Canada, 2021, pp. 1-5

(5) Y. Wang, H. Zhang and F. Lu, "Review, Simulation, and Design of Four Basic CPT Topologies and the Application of High-Order Compensation Networks," in IEEE Transactions on Power Electronics, vol. 37, no. 5, pp. 6181-6193, May 2022

(6) H. Namiki, T. Imura and Y. Hori, "Magnetic Field Resonant Coupling in Wireless Power Transfer Comparison of Multiple Circuits Using LCL," 2022 IEEE 7th Southern Power Electronics Conference (SPEC), Nadi, Fiji, 2022, pp. 1-6

(7) X. Dai, Y. Huang and Y. Li, "Topology comparison and selection of wireless power transfer system and parameter optimization for high voltage gain," 2017 IEEE PELS Workshop on Emerging Technologies: Wireless Power Transfer (WoW), Chongqing, China, 2017, pp. 1-5

(8) S. Luo, S. Li and H. Zhao, "Reactive power comparison of four-coil, LCC and CLC compensation network for wireless power transfer," 2017 IEEE PELS Workshop on Emerging Technologies: Wireless Power Transfer (WoW), Chongqing, China, 2017, pp. 268-271

(9) S. Li, W. Li, J. Deng, T. D. Nguyen and C. C. Mi, "A Double-Sided LCC Compensation Network and Its Tuning Method for Wireless Power Transfer," in IEEE Transactions on Vehicular Technology, vol. 64, no. 6, pp. 2261-2273, June 2015

(10) A. Mahesh, B. Chokkalingam and L. Mihet-Popa, "Inductive Wireless Power Transfer Charging for Electric Vehicles–A Review," in IEEE Access, vol. 9, pp. 137667-137713, 2021

(11) Y. Li et al., "High Efficiency WPT System for Electric Vehicles with LCL-S and SS compensation," 2019 IEEE 4th International Future Energy Electronics Conference (IFEEC), Singapore, 2019, pp. 1-4

(12) S. Sasikumar and K. Deepa, "Comparative Study of LCL-S and LCC-S Topology of Wireless EV charging System," 2019 Innovations in Power and Advanced Computing Technologies (i-PACT), Vellore, India, 2019, pp. 1-6

(13) H. Namiki, T. Imura and Y. Hori, "Characteristic Comparison of 16 Circuits for Inductive Power Transfer," 2023 IEEE Wireless Power Technology Conference and Expo (WPTCE), San Diego, CA, USA, 2023, pp. 1-6

(14) S. Cruciani, T. Campi, F. Maradei and M. Feliziani, "Simulation of Compensation Networks for a Transcutaneous WPT System to Achieve Compliance with ICNIRP Basic Restrictions," 2021 IEEE International Joint EMC/SI/PI and EMC Europe Symposium, Raleigh, NC, USA, 2021, pp. 381-385

(15) S. Kuroda and T. Imura, "Derivation and Comparison of Efficiency and Power in Non-resonant and Resonant Circuit of Capacitive Power Transfer," 2020 IEEE PELS Workshop on Emerging Technologies: Wireless Power Transfer (WoW), Seoul, Korea (South), 2020, pp. 152-157

(16) L. Pamungkas, S. -H. Wu and H. -J. Chiu, "Equivalent Circuit Approach for Output Characteristic Design of Capacitive Power Transfer," in IEEE

Transactions on Circuits and Systems II: Express Briefs, vol. 68, no. 7, pp. 2513-2517, July 2021
(17) B. Luo, L. Xu, T. Long, Y. Xu, R. Mai and Z. He, "An LC-CLC Compensated CPT System to Achieve the Maximum Power Transfer for High Power Applications," 2020 IEEE Applied Power Electronics Conference and Exposition (APEC), New Orleans, LA, USA, 2020, pp. 3186-3189
(18) C. Xia, R. Chen, Y. Liu, G. Chen and X. Wu, "LCL/LCC resonant topology of WPT system for constant current, stable frequency and high-quality power transmission," 2016 IEEE PELS Workshop on Emerging Technologies: Wireless Power Transfer (WoW), Knoxville, TN, USA, 2016, pp. 110-113
(19) F. Lu, H. Zhang, H. Hofmann and C. Mi, "A Double-Sided LCLC-Compensated Capacitive Power Transfer System for Electric Vehicle Charging," in IEEE Transactions on Power Electronics, vol. 30, no. 11, pp. 6011-6014, Nov. 2015
(20) S. Wang, J. Liang and M. Fu, "Simulation and Design of Capacitive Power Transfer Systems Based on Induced Voltage Source Model," in IEEE Transactions on Power Electronics, vol. 35, no. 10, pp. 10532-10541, Oct. 2020
(21) S. Sinha, A. Kumar, B. Regensburger and K. K. Afridi, "Design of High-Efficiency Matching Networks for Capacitive Wireless Power Transfer Systems," in IEEE Journal of Emerging and Selected Topics in Power Electronics, vol. 10, no. 1, pp. 104-127, Feb. 2022
(22) B. Luo, A. P. Hu, H. Munir, Q. Zhu, R. Mai and Z. He, "Compensation Network Design of CPT Systems for Achieving Maximum Power Transfer Under Coupling Voltage Constraints," in IEEE Journal of Emerging and Selected Topics in Power Electronics, vol. 10, no. 1, pp. 138-148, Feb. 2022
(23) H. Zhang, F. Lu, H. Hofmann, W. Liu and C. C. Mi, "A Four-Plate Compact Capacitive Coupler Design and LCL-Compensated Topology for Capacitive Power Transfer in Electric Vehicle Charging Application," in IEEE Transactions on Power Electronics, vol. 31, no. 12, pp. 8541-8551, Dec. 2016
(24) H. Zhang, F. Lu, H. Hofmann, W. Liu and C. C. Mi, "Six-Plate Capacitive Coupler to Reduce Electric Field Emission in Large Air-Gap Capacitive Power Transfer," in IEEE Transactions on Power Electronics, vol. 33, no. 1, pp. 665-675, Jan. 2018
(25) X. Wu, Y. Su, X. Hou, X. Qing and W. Zhu, "Load Adaptation of Capacitive Power Transfer System with a Four-Plate Compact Capacitive Coupler," 2019 IEEE PELS Workshop on Emerging Technologies: Wireless Power Transfer (WoW), London, UK, 2019, pp. 324-329
(26) S. Ning, J. Yang, Q. Zhu, M. Su, R. Tan and Y. Liu, "Comparative Simulation of LCL, LCLC, CLLC Compensation Networks for Capacitive Power Transfer," 2018 IEEE 4th Southern Power Electronics Conference (SPEC), Singapore, 2018, pp. 1-6
(27) J. Dai and D. C. Ludois, "Single Active Switch Power Electronics for Kilowatt Scale Capacitive Power Transfer," in IEEE Journal of Emerging and Selected Topics in Power Electronics, vol. 3, no. 1, pp. 315-323, March 2015
(28) M. S. Mazli et al., "Inductive & Capacitive Wireless Power Transfer System," 2018 7th International Conference on Computer and Communication Engineering (ICCCE), Kuala Lumpur, Malaysia, 2018, pp. 307-312
(29) Z. Zhang, H. Pang, A. Georgiadis and C. Cecati, "Wireless Power Transfer—An Overview," in IEEE Transactions on Industrial Electronics, vol. 66, no. 2, pp. 1044-1058, Feb. 2019
(30) J. Dai and D. C. Ludois, "A Survey of Wireless Power Transfer and a Critical Comparison of Inductive and Capacitive Coupling for Small Gap Applications," in IEEE Transactions on Power Electronics, vol. 30, no. 11, pp. 6017-6029, Nov. 2015
(31) H. Namiki, T. Imura and Y. Hori, "Comparison of Multiple Circuits Including LCL in Inductive Power Transfer and Capacitive Power Transfer," IECON 2023- 49th Annual Conference of the IEEE Industrial Electronics Society, Singapore, Singapore, 2023, pp. 1-7

Hirono Namiki

(Non-Member) She entered the Department of Electrical Engineering, Faculty of Science and Technology, Tokyo University of Science in April 2018, graduated in March 2022, and entered the Department of Electrical Engineering, Graduate School of Science and Technology, Tokyo University of Science in April 2022. She is currently focusing on the unified theory of Inductive Power Transfer and Capacitive Power Transfer. She is a student member of the Institute of Electrical and Electronics Engineers (IEEE).

Takehiro Imura (Member) Received the bachelor's degree in electrical and electronics engineering from Sophia University, Tokyo, Japan,

in 2005, and the M.E. degree in electronic engineering and the D.Eng. degree in electrical engineering from the University of Tokyo, Tokyo, in 2007 and 2010, respectively. He joined the Department of Advanced Energy, Graduate School of Frontier Sciences, the University of Tokyo, as a Research Associate, where since 2015, he has been a Project Lecturer. In 2019, he joined the Department of Electrical Engineering, Tokyo University of Science, as an Associate Professor. He is currently investigating wireless power transfer using magnetic resonant coupling and electric resonant coupling. His research interests include electric vehicle in-motion connected to renewable energy, sensors and cancer treatment. He is the winner of the IEEJ Industry Applications Society Distinguished Transaction Paper Award in 2015, of the IEEE Power Electronics Transactions First Prize Paper Award in 2017. He is a member of the Institute of Electrical and Electronics Engineers (IEEE), the Institute of Electronics, Information and Communication Engineers (IEICE), and the Society of Automotive Engineers of Japan (JSAE).

Yoichi Hori

(Fellow) Yoichi Hori received his B.S., M.S., and Ph.D. degrees in Electrical Engineering from the University of Tokyo, Tokyo, Japan, in 1978, 1980, and 1983, respectively. In 1983, he joined the Department of Electrical Engineering, The University of Tokyo, as a Research Associate. He later became an Assistant Professor, an Associate Professor, and, in 2000, a Professor at the same university. In 2002, he moved to the Institute of Industrial Science as a Professor in the Information and System Division, and in 2008, to the Department of Advanced Energy, Graduate School of Frontier Sciences, the University of Tokyo. He retired in March 2021, and has been in current position since April. Professor Emeritus of the University of Tokyo. From 1991-1992, he was a Visiting Researcher at the University of California at Berkeley. His research fields are control theory and its industrial applications to motion control, mechatronics, robotics, electric vehicles, etc. Recently, he has also been focusing on the research and promotion of wireless power transfer. He is a Life Fellow of IEEE (the Institute of Electrical and Electronics Engineers) and a past AdCom member of IES (Industrial Electronics Society). He has been the Treasurer of the IEEE Japan Council and Tokyo Section in a few years since 2001.